MINERALOGICAL MAGAZINE, VOL. 45, 1982, PP. 101-6

Trace element distributions between the perthite phases of alkali feldspars from pegmatites

R. A. MASON*

Department of the Geophysical Sciences, University of Chicago, Chicago, Illinois 60637 USA

ABSTRACT. The distribution of various trace elements between the K-feldspar and albite phases of perthites from several pegmatites was determined by ion microprobe. Ranges in distribution coefficients (wt. % in K-feldspar/wt. % in albite) are: Li, 1.2–780; Mg, 0.2–1.1; P, 0.1–17; Ca, 0.02–1.6; Cs, 32–820; Ba, 24–284; Pb, 1.6–30; Fe, 0.3–0.7; Rb, 59–5505; Sr, 1.3–5.1. The trace elements are zoned within the K-feldspar lamellae and the profiles are interpreted as the result of cross coefficients in the diffusion matrix.

THE distribution of trace elements between the albite and K-feldspar phases of perthites has been determined as part of a study of the trace element patterns of feldspars from zoned pegmatites. Any trace elements with strong dependence of distribution coefficients on pressure or temperature would be useful for geothermometry and geobarometry. This would be particularly helpful in pegmatites where feldspar phase compositions are constrained by the almost vertical limbs of the alkali feldspar solvus at low temperature (Smith and Parsons, 1974; Goldsmith and Newton, 1974) and thus provide little temperature information.

Early work on samples from Vežňa, Czechoslovakia (provided by P. Černy) indicated strong partitioning and zoning within lamellae and was reported in abstract (Mason, 1980). In order to investigate this more thoroughly a small suite of pegmatitic samples has been studied. The samples were chosen for their coarseness; unfortunately two are from unknown localities but the large size of the single crystals and the coarseness of the lamellae leave no doubt that they are pegmatitic in origin. Table I gives details of specimens studied.

Experimental techniques. The coarsest samples were cut both parallel to and perpendicular to the perthite lamellae; finer specimens were only sectioned parallel to the lamellae. Fragments of the slices were then mounted in epoxy on a silica glass slide together with samples of alkali feldspars which are used as ion microprobe standards. The slide was then polished and carbon coated.

* Present address: Department of Earth Sciences, Bullard Laboratories, Madingley Rise, Cambridge CB3 0EZ.

Following light optical inspection the slide was examined with a scanning electron microscope operating in the backscattered electron mode, the contrast in the image being formed as a result of the difference in mean atomic weight of the intergrown albite and K-feldspar. This method of observation was preferred to optical examination because the latter does not discriminate sufficiently well between lamellae at the surface and those at some depth within the specimen. Photographs of areas of interest were made and subsequently used to locate points for electron and ion probe analysis. Routine major element analyses were made by energy-dispersive electron microprobe methods using an accelerating voltage of 15 kV and beam current of 0.1 μA. Minor elements were determined by wavelength-dispersive methods using an accelerating voltage of 25 kV and beam current of 0.4 μA. The beam diameter was 30 μm in both cases.

Additional analyses of potassium in the K-feldspar at the lamellar boundaries were made by energy dispersive analysis under the following conditions: 15 kV, 0.5 μA; beam diameter 2 μm. Position relative to the perthite boundary was judged by the appearance and disappearance of the electron-excited luminescence in the K-feldspar. About ten points were analysed at each distance from the boundary. The electron probe was used in preference to the ion probe because the very high ^{41}K count rate expected would cause damage to the detector.

Following electron probe analysis the sample was cleaned and coated with gold in preparation for ion probe analysis. The following instrumental settings were used: $^{16}O^-$ primary beam; 10 nA beam current; 20 kV accelerating voltage; 20 μm beam diameter. Molecular interferences are present at some mass numbers (e.g. $^{40}Ca^{16}O^+$ at M/e = 56) so the trace elements were

TABLE I. *Details of specimens*

Name	Locality	Profile and figure numbers
Nine	unknown	1*a*, cut perpendicular to lamellae (fig. 1)
Nine	unknown	1*b*, cut parallel to lamellae (not plotted)
Middletown	Delaware Co. Pa	2*a*(1) and (2) cut perpendicular to lamellae (figs. 2 and 3)
Middletown	Delaware Co. Pa	2*b*, cut parallel to lamellae (fig. 4)
80	unknown	3, cut perpendicular to lamellae (fig. 5)
Pellotsalo	USSR (formerly Finland)	4, cut parallel to lamellae (fig. 6)

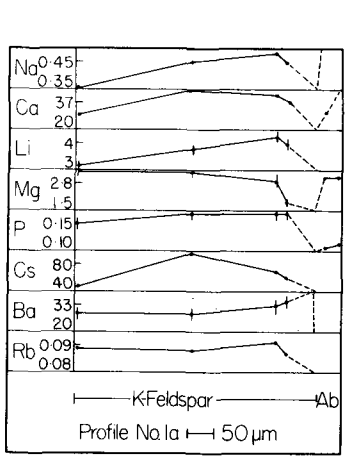

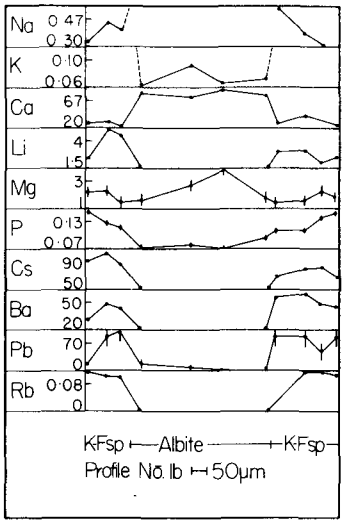

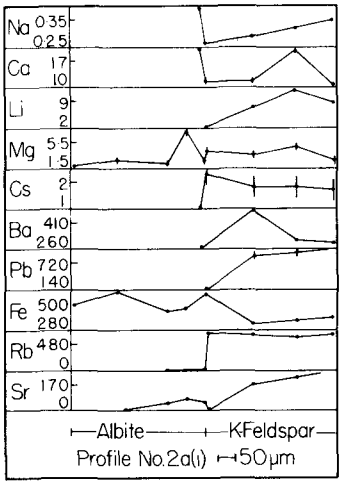

FIGS. 1–3. FIG. 1 (*left*). Trace element profile 1*a*. FIG. 2 (*centre*). Profile 1*b*. FIG. 3 (*right*). Profile 2*a*(1). Na, K, and P in wt. %; others in ppmw except Rb which is in wt. % in figs. 1 and 2, and in ppmw in fig. 3.

analysed in two sets: ^{7}Li, ^{24}Mg, ^{31}P, ^{40}Ca, ^{133}Cs, ^{138}Ba, and ^{208}Pb, which are interference free, were analysed at low mass resolution. ^{56}Fe, ^{85}Rb, and ^{88}Sr were analysed at high mass resolution to avoid molecular interferences. Several standard feldspars were checked at intervals to confirm instrumental stability. The standards were previously analysed by electron probe or, in the case of Li and B, by chemical methods. (E. E. Foord kindly provided samples and analyses). Details of electron and ion probe standards are given by Mason *et al.* (1982). Ion and electron probe analyses made at the same location on the unknown were in good agreement.

Results. Table II gives analytical results; sample numbers correspond to those in Table I. Major elements are given as Or + Ab + An = 100 mole % and minor elements in ppm by weight as determined by ion probe. The minor elements are the averages of all the determinations made on each phase and are used to calculate distribution coefficients, D = wt. % in K-feldspar/wt. % in albite.

As noted above, the early work indicated zonation of trace elements within lamellae and the present more detailed study confirms this. Figs. 1–6 show the profiles for the minor elements, which are plotted as wt. % or ppmw. Profile 2*b* is not presented because the highly irregular perthite boundary encountered rendered it complex. Values in Table II for profile 2*b* are averaged from those points which are sufficiently far from the boundary to be uncontaminated by the 'wrong' phase. The position of the perthite boundaries are marked at the base of each diagram. Error bars, where shown,

Table II.

Sample/traverse No.	1a			1b			2a(1)			2a(2)			2b			3.			4.			Range in D
	Or	Ab	D	Or	Ab	D	Or	Ab	D	Or	Ab	D	Or	Ab	D	Or	Ab	D	Or	Ab	D	
Or mole %	92	2		95	99		96	0.8		96	0.8		95	0.6		95	1		95	1.3		
Ab "	8	98		5	1		4	98.6		4	98.6		5	98.8		5	99		5	97.7		
An "	-	-		-	-		-	0.6		-	0.6		-	0.6		-	-		-	1.0		
Li ppmw	4.0	0.05	80	3.1	0.06	52	7.4	0.07	106	6.1	0.02	305	3.0	0.3	10	7.8	0.01	780	0.16	0.13	1.2	1.2 - 780
Mg "	2.9	3.2	0.91	1.8	2.5	0.72	3.7	3.3	1.1	4.1	10	0.4	2.0	8.7	0.2	2.4	3.0	0.8	2.8	7.4	0.4	0.2 - 1.1
P "	1600	1082	1.5	2028	932	2.2	7	12	0.6	10	15	0.7	6	51	0.1	2217	162	14	770	44	17	0.1 - 17
Ca "	38	94	0.4	24	73	0.3	18	728	0.02	21	639	0.03	16	718	0.02	22	14	f.6	53	1350	0.04	0.02 - 1.6
Cs "	68	0.87	78	82	0.1	820	1.9	0.05	38	1.9	0.06	32	2.0	0.05	40	37	0.5	80	12	0.07	171	32 - 820
Ba "	31	1	31	50	0.3	167	341	1.2	284	383	7	55	310	3	103	12	0.1	120	307	13	24	24 - 284
Pb "	n.a.	n.a.	-	76	13	5.9	729	114	6.4	842	220	3.8	698	432	1.6	74	2.5	30	73	13	5.6	1.6 - 30
Fe "	<1	<1	-	<1	<1	-	343	514	0.7	288	936	0.3	202	341	0.6	<1	<1	-	<1	<1	-	0.3 - 0.7
Rb "	915	0.3	3052	1101	0.2	5505	654	1.5	436	593	10	59	588	1.3	452	1808	2.2	822	802	6.6	122	59 - 5505
Sr "	<1	<1	-	<1	<1	-	216	42	5.1	157	121	1.3	n.a.	n.a.	-	<1	<1	-	<1	<1	-	1.3 - 5.1

n.a. = not analysed.

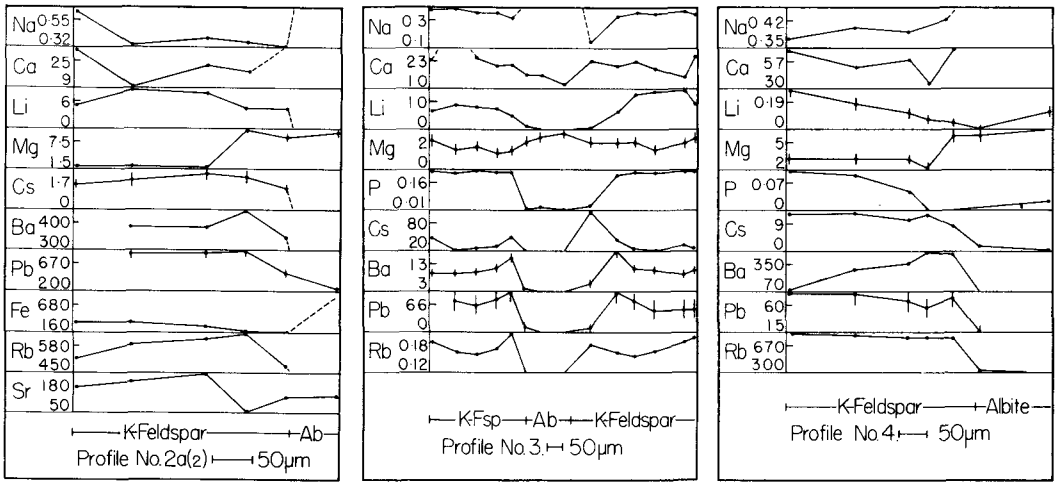

FIGS. 4–6. FIG. 4 (*left*). Trace element profile 2*a*(2). FIG. 5 (*centre*). Profile 3. FIG. 4 (*right*). Profile 4. Na and P wt. %; others in ppmw except Rb which is in wt. % in fig. 5 and ppmw in figs. 4 and 6.

are calculated from the count rate and are plotted at the 2σ level. Absence of error bars means that the 2σ errors are smaller than the plotting symbol. Dotted lines indicate uncertainty. Note that in many cases element concentrations in the sodic phase are substantially below the base line drawn for each element.

Li, Cs, Ba, Pb, and Rb are partitioned into the K-phase but the apparent distribution coefficients vary widely (Table II). Mg is mostly partitioned into the sodic phase but the values determined on sample 2 are responsible for the whole range in apparent D's in Table II. Values from the other specimens are in the range 0.4–0.9. P is partitioned into the K-feldspar phase except in sample 2 (D = 0.1–0.6) which also has the lowest P contents of the suite. Ca is partitioned into the sodic phase except in sample 3 which has the lowest Ca content and a D value of 1.6. Fe is present above ~ 1 ppmw only in sample 2 in which it is partitioned into the sodic phase. Sr is present only in specimen 2 and is partitioned into the potassic phase.

Casual perusal of figs. 1–6 shows that the minor element profiles across lamellae are not horizontal as they should be at equilibrium (fig. 7*a*). Undoubtedly this non-equilibrium distribution contributes to the range of D values given in Table II. Closer inspection reveals that there are certain features in the profile shapes that are systematic and fairly consistent among the samples. Li illustrates this particularly well. In five of the six profiles Li reaches a maximum concentration in the K-feldspar at some distance away from the lamellar boundary. The distance from the boundary at which this maximum occurs varies from ~ 90–330 μm among the five samples and may not be symmetrical with respect to either distance or concentration on each side of the sodic lamella (e.g. fig. 2). In the profile for sample 4 (fig. 6) there is a very clear decline in Li content towards the boundary; there may well be a maximum beyond the limit of the profile (250 μm from the boundary). Ba, Cs, Rb, and Pb show analogous behaviour, though less consistently in the case of Rb and Pb. In two out of four profiles P declines towards the K-feldspar/albite boundary; in the others it remains constant up to the boundary.

The elements which substitute into the sodic phase are less consistent in their behaviour. Mg avoids the area adjacent to the boundary in the K-phase in specimens 1*a* and 1*b* (figs. 1 and 2) but this behaviour is reversed in profiles 2*a*(2) and 4 (figs. 3 and 6). Ca reaches a maximum in the K-feldspar away from the boundary in three of the six profiles but is erratic in the others. Fe was determined with precision only in three profiles (sample 2); it behaves unsystematically in profile 2*a*(1) but shows a clear decline towards the lamellar boundary before increasing dramatically within the albite lamella. Sr was present only in sample 2; apparently it behaves erratically.

Discussion. In interpreting the profiles it is assumed that the perthites are the result of unmixing, not replacement. In support of this both the hand specimen and SEM inspection showed that all the samples are intergrowths having a regular orientation and are not of the 'patch' perthite type which may indicate replacement.

Fig. 7 shows the element profiles to be expected under equilibrium (7*a*) and non-equilibrium conditions (7*b*). The solid line is for an element partitioned into the potassic phase and the dashed line for an element partitioned into the sodic phase. At equilibrium each element, major or minor, should be distributed homogeneously within each phase. Fig. 7*b* is the profile expected at some stage between the inception of unmixing and final equilibration.

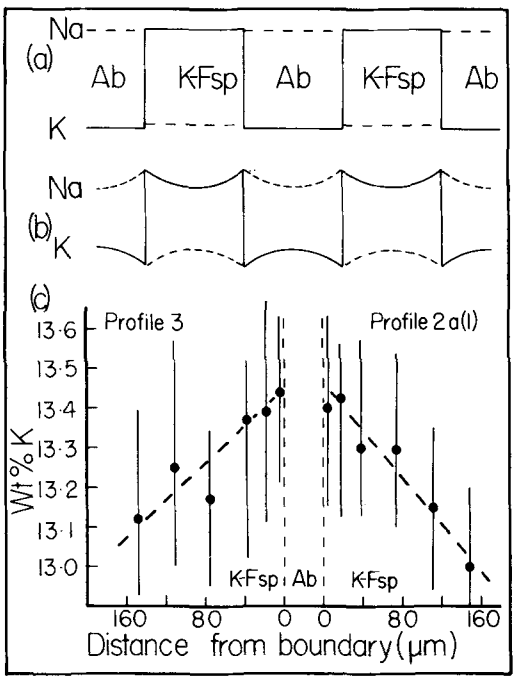

FIG. 7. Theoretical diffusion profiles and experimental potassium profiles in samples 3 and 2*a*(1).

Elements partitioning into the potassic phase are expelled from the sodic phase and accumulate at the boundary to produce the 'M' type profile commonly shown by Ni in the kamacite–taenite intergrowths of meteorites (e.g. Wood, 1964). Fig. 7*c* shows experimental potassium profiles determined on samples 2*a*(1) and (3). The error bars represent the maximum and minimum values observed at each distance from the boundary. Although the errors are large there is a clear decrease in K-content on moving further into the K-phase. Similar results are reported by Smith (1974, vol. 2, p. 460). This 'M' profile results from a decreasing effective diffusion distance for K as temperature falls, and demonstrates lack of equilibrium. This is despite the fact that diffusion rates for K in albite are lower than for K in potassium feldspar (Petrović, 1974, and data summarized by Smith, 1974, vol. 2). Several of the sodium profiles behave in the manner depicted by the dashed lines of fig. 7*b*, i.e. decreasing toward the albite–K-feldspar boundary before increasing rapidly in the albite phase. The two profiles which do not show this behaviour are more difficult to interpret (profile 1*b*, in part, and profile 4). A re-heating event would produce the observed effect but can be ruled out since sample 1*a*, which is equivalent to 1*b* in all but section orientation, shows the expected behaviour.

Any element partitioning into the potassic phase (Li, Cs, Ba, Pb, and Rb) should show the same behaviour as K—reaching a maximum concentration adjacent to the boundary. If the results of mineral/melt partitioning experiments (Long, 1978) can be extended to the present case we should expect to see Ba, for example, concentrated in the purest K-feldspar, i.e. at the boundary.

Three hypotheses may be considered to explain the behaviour of those elements which show concentration maxima displaced from the boundary:

1. Leaching has removed trace elements from the perthite boundary. Nagy and Giletti (1980) have shown that in perthitic alkali feldspars there is enhanced transport of ^{18}O along the perthite boundaries implying non-volume diffusion of an oxygen-bearing species. Any fluid phase penetrating along the boundary may leach trace elements from the boundary region more rapidly than in more distant portions of a lamella. This process is unlikely to have operated in the present case because the major element profiles are undisturbed and there are no signs of alteration along the lamellar boundaries.

2. Defects concentrated at the interface may lead to enhanced diffusion rates and consequent 'pile up' away from the boundary. This hypothesis is not favoured because transmission electron microscope studies of mineral exsolution show that defects concentrate within about 1 μm of lamellar boundaries rather than the hundreds of μm required in the present case (e.g. Lally *et al.*, 1976). Also we should not expect to see the 'M' profile for potassium retained.

3. Maxima in the concentration profiles result from coupling of the diffusion rates of the minor elements to those of the major elements. This hypothesis is considered below.

Binary diffusion should give rise to profiles such as depicted in fig. 7*b*. In the special case of binary diffusion the chemical potential gradients of the diffusing species can be assumed to be independent if the system shows only a small departure from equilibrium (Glansdorff and Prigogine, 1971). In

the case of multicomponent diffusion a more general form of the flux equation must be used:

$$J_1 = -M_{11}\frac{du_1}{dx} - M_{12}\frac{du_2}{dx} - M_{13}\frac{du_3}{dx}$$

$$J_2 = -M_{21}\frac{du_1}{dx} - M_{22}\frac{du_2}{dx} - M_{23}\frac{du_3}{dx}$$

$$J_3 = -M_{31}\frac{du_1}{dx} - M_{32}\frac{du_2}{dx} - M_{33}\frac{du_3}{dx}$$

in which the J's are fluxes of components 1, 2, and 3; the M's are coefficients analogous to diffusion coefficients: the u's are chemical potentials and x is a diffusion direction (see for example Shewmon, 1963, p. 122). The assumption of independence of chemical potential gradients in the binary case means taking the cross terms (M_{12}, M_{21}) as zero. In the case of multicomponent diffusion this assumption is strictly invalid though it is a matter of experiment to determine the magnitude of their effect. Loomis (1978*a* and *b*) has shown that they must be taken into account in modelling the diffusion profiles of minor components in garnet. Intuitively the cross terms can be visualized as reflecting difference in diffusion rates of the major elements, in this case K and Na. During unmixing K and Na diffuse in opposite directions and at different rates. Since the net flux of matter across any arbitrary plane in the crystal must be equal to zero, a charge, mass, and volume deficiency is avoided by diffusion of the minor components towards those regions where such a deficiency may arise, i.e. the minor elements diffuse in response to the chemical potential gradients of the major elements. In garnet the cross terms for minor components may be larger than the diagonal terms of the diffusion matrix (Loomis 1978*b*). The difference in diffusion rates for Na and K amounts to about two orders of magnitude, at least near 700 °C (Foland, 1972, reported in Smith, 1974). This difference is considered to be responsible for the observed peaking of trace element concentrations away from the albite–K-feldspar boundary.

Although the profiles described above do not represent equilibrium it is worthwhile briefly considering the partition coefficients themselves. Fig. 8 shows an Onuma diagram (Onuma *et al.*, 1968; Philpotts, 1978) for profile 2*a*(1); it was selected because data are available for more elements in this sample than any other. Round symbols are for monovalent cations, squares for divalent cations and triangles for those elements expected to substitute into tetrahedral sites. Ionic radii are from Shannon and Prewitt (1969). The general features of the diagram are representative of the Onuma diagram for the other samples. There are differences in detail however. For example in samples 3 and 4 the 'slope' of the line connecting Ba, Pb, and Ca is not as similar to that connecting K–Na as in fig. 8; also in sample 4 the maximum partition coefficient for a univalent cation is for K, not Rb, as is the case in all other samples.

In principle if the trace elements are substituting in lattice sites and not defects it should be possible to draw smooth curves connecting cations of equal valence (Philpotts, 1978). Those cations most suitable for a given site in terms of ionic radius should show the largest partition coefficients with values of D declining at ionic radii larger and smaller than optimum. In drawing curves through the data in fig. 8 I have followed Philpotts (1978) in supposing that the lines for the univalent divalent cations should be at least quasi-parallel. With these subjective judgements borne in mind the following remarks can be made:

1. The general features are as expected with a maximum occurring for one particular ionic radius (Rb, exception noted above) implying substitution of trace elements in lattice sites rather than in defects.
2. Partition coefficients for Li and Mg are anomalous.

That the maximum partition coefficient is for Rb rather than the major element, K, is unexpected and suggests that Rb is more suitable in terms of radius in the M site of a K-feldspar than is the 'host' cation, K! This in turn implies that there is

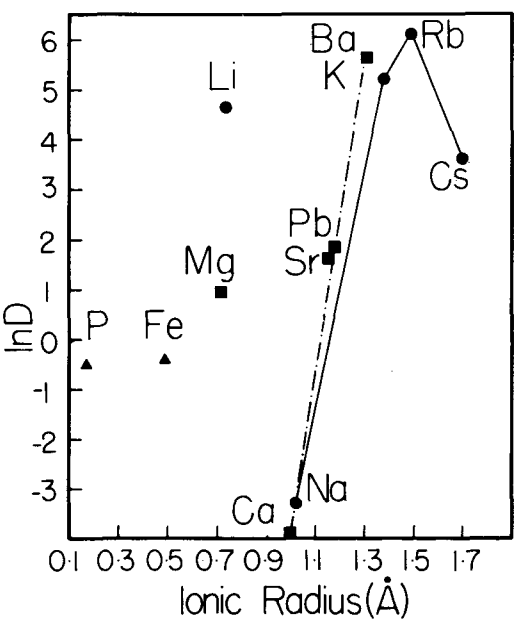

FIG. 8. 'Onuma' diagram for profile 2*a*(1).

more distortion of the Al,Si framework involved in accommodating K rather than Rb in the *M* site. Indirect confirmation of this view comes from the observations of Gordienko and Kamentsev (1969) that increasing substitution of Rb (and Cs) inhibits the orthoclase–microcline transition. Note that the larger values of *D* for Rb rather than K cannot be attributed to the effect of the shape of the profiles; Rb is one of the cations which shows the diffusion effects less consistently than any of the others, i.e. the profiles are flatter than for the other elements.

The suggestion that the Li distribution coefficients are anomalous is supported by comparison with the data in Smith (1974) which show that Li generally substitutes preferentially into the plagioclase of coexisting plagioclase–K-feldspar pairs. Li is the cation showing the diffusion effects described above most consistently and undoubtedly the anomaly in the Onuma diagrams is exaggerated slightly by this effect. However, even when the lowest observed Li concentration in the K phase is used in calculation of the partition coefficients there is still a clear anomaly, *D*(K-feldspar/albite) is > 1 for all except sample 4 and even here the distribution coefficient is still substantially larger than would be predicted from the trend for univalent cations on the Onuma diagram.

The cause of this anomaly is unclear. Perhaps the effect of cross coefficients on the diffusion of Li is sufficiently strong that the chemical potential gradient down which it diffuses is actually reversed in direction compared with the intrinsic chemical potential gradient of Li. An alternative explanation may be that Li occupies some sort of distorted *M* site, the distortion being caused by the presence of other trace elements. In support of this a plot of the log D_{Li} versus the total concentration of trace elements in the *M* site of the K-feldspar shows a good correlation though the profiles for sample 1 violate the relationship. Similar explanations may perhaps apply to the apparent Mg anomaly.

Those elements showing the widest ranges of partition coefficients and which are present in both phases in easily measurable concentrations would be the most promising for investigation as geothermometers. The widest ranges in D are shown by Li(1.2–780), P(0.1–17), and Rb(59–5505) (see Table II). This may be due to the complexities of the profile shapes especially for Li, because the variation within a single sample (no. 2) is large. Phosphorous is present in readily measurable quantities in both phases and shows moderate variation in a single sample and may be worthy of an experimental investigation. The remaining elements are either present in too low concentrations, show too much variation in a single sample or have only narrow ranges of partition coefficient.

Acknowledgements. J. R. Goldsmith, E. E. Foord, A. J. Irving, and C. Solomon provided samples which were used as ion probe standards. I. M. Steele, R. Draus, I. Baltuska and O. Draughn provided valuable technical assistance. G. D. Price and J. V. Smith read and criticized the manuscript. The work was supported by NSF grant 77-27100 EAR to J. V. Smith.

REFERENCES

Foland, K. A. (1972) Abstr. 2.8. Program for Advanced Study Institute on Feldspars. July 1972. Manchester.

Glansdorff, P., and Prigogine, I. (1971) *Thermodynamic Theory of Structure, Stability and Fluctuations.* (Wiley).

Goldsmith, J. R., and Newton, R. C. (1974) In *The Feldspars* (W. S. MacKenzie and J. Zussman, eds.), Manchester Univ. Press, 337–59.

Gordienko, V. V., and Kamentsev, I. Ye. (1969) *Geochem. Int.* **6,** 180–92.

Lally, J. S., Heuer, A. H., and Nord, G. L., *Jr.* (1976) In *Electron Microscopy in Mineralogy* (H.-R. Wenk *et al.*, eds.), Springer, Heidelberg, 214–19.

Long, D. E. (1978) *Geochim. Cosmochim. Acta,* **42,** 833–46.

Loomis, T. P. (1978*a*) *Am. J. Sci.* **278,** 1099–118.

——(1978*b*) Ibid. **278,** 1119–37.

Mason, R. A. (1980) *Geol. Soc. Am. Abstr. with programs* **12,** (7), 477.

——Smith, J. V., Dawson, J. B., and Treves, S. B. (1982) *Mineral. Mag.* **46,** 7–11.

Nagy, K., and Giletti, B. J. (1980) *Geol. Soc. Am. Abstr. with programs,* **12,** (7), 490.

Onuma, N., Higuchi, H., Wakita, H., and Nagasawa, H. (1968) *Earth Planet. Sci. Lett.* **5,** 47–51.

Petrović, R. (1974) In *The Feldspars* (W. S. MacKenzie and J. Zussman, eds.), Manchester Univ. Press, 174–82.

Philpotts, J. A. (1978) *Geochim. Cosmochim. Acta,* **42,** 909–20.

Shannon, R. D., and Prewitt, C. T. (1969) *Acta Crystallogr.* **B25,** 925–46.

Shewmon, P. G. (1963) *Diffusion in Solids.* McGraw-Hill, New York.

Smith, J. V. (1974) *Feldspar Minerals,* vol. 2. Springer, Heidelberg.

Smith, P., and Parsons, I. (1974) *Mineral. Mag.* **39,** 747–67.

Wood, J. A. (1964) *Icarus* **3,** 429–59.